Analysis of Skeletal Phenotypes of Matrix-Gla Protein (MGP) and Twisted Gastrulation (Twsg1) Deficient Mice

A THESIS
SUBMITTED TO THE FACULTY OF THE GRADUATE SCHOOL
OF THE UNIVERSITY OF MINNESOTA
BY

Ann Elizabeth Emery

IN PARTIAL FULFILLMENT OF THE REQUIREMENTS
FOR THE DEGREE OF
MASTER OF SCIENCE

Rajaram Gopalakrishnan B.D.S, PH.D, Advisor

August 2010

ACKNOWLEDGEMENTS

I would like to first thank my advisor and mentor, Dr Rajaram Gopalakishnan, for support and guidance while in the Oral Biology Graduate Program. His support has been invaluable in this project. Working with him has been a great experience both personally and professionally, and I have grown as a scientist as a result of being in his lab.

Additional appreciation goes to Dr Kim Mansky for her assistance with helping to complete this program, understand results, and troubleshoot problems in the research. Her patience and support has been very helpful these past three years.

I would like to also acknowledge the support of the Genetics, Cell Biology and Development faculty members Dr Hiroshi Nakato who has been a positive addition to my committee, and Dr Anna Petryk who has also been mentor for me these past few years and challenged me to be a better scientist. Additional appreciation to the Oral Biology faculty and staff including Dr Mark Herzberg and the steering committee who welcomed feedback and provided support in navigating the program and requirements.

Deepest gratitude and thanks to the current and past members of the Gopalakrishnan and Mansky lab including Dr Eric Jensen, Lan Pham, and Julio Sotillo. They have challenged me to be a better scientist and made coming to the lab everyday very enjoyable. Also, I would like to thank my family and husband for support and encouragement to reach my goals.

Ann Emery
2010

DEDICATION

This thesis is dedicated to the skeletal biologists of the Gopalakrishnan and Mansky lab who through their hard work and persistence seek to cure diseases of bone remodeling including osteoporosis.

ABSTRACT

Matrix Gla-Protein (MGP) and Twisted Gastrulation (Twsg) are secreted proteins that reside in the extracellular matrix. MGP is a potent inhibitor of mineralization in both soft- and hard- tissues. $MGP^{-/-}$ mice exhibit numerous abnormalities, the most severe being aortic calcification that leads to death by approximately two months of age. Despite extensive studies using cartilage and cardiovascular tissues in these mice, little is known about how MGP deficiency affects bone development, specifically the impact on osteoblasts and osteoclasts. Twisted Gastrulation is a modulator of BMP signaling in many tissues. Twsg1 deficient mice exhibit several phenotypes including craniofacial, salivary gland defects, and skeletal defects. Twsg1 has also been implicated in embryo patterning and cartilage development but to date, there has been no study of the bone in these mice. Preliminary analysis using faxitron (x-ray) analysis of MGP and Twsg1 wild type and homozygous deficient mice revealed reduced bone and an osteopenic bone phenotype. The goal of my thesis project was to characterize 1) the *in vivo* (both dynamic and static) phenotype of $Twsg^{-/-}$ mice and 2) both *in vivo* and *in vitro* (static) skeletal phenotype of $MGP^{-/-}$ mice. Using microcomputer tomography (μCT), both static, and in the case of Twsg1, dynamic, histomorphometric analysis was performed to characterize the skeletal phenotype in the animals. In both mouse models there was a significant decrease in both cortical and trabecular bone present. Primary osteoblasts and osteoclasts were used to further characterize the *in vitro* phenotype in the $MGP^{-/-}$ mouse model. Primary osteoblasts showed premature mineralization and differentiation. Bone sialoprotein (BSP) and osteoclacin (OCN) mRNA levels were both elevated. Surprisingly, osteoclast differentiation also showed enhancement with increased number and larger multinuclear TRAP+ osteoclasts. They also showed increases in DC-STAMP and TRAP mRNA levels compared to the wild type animals. The data collected in this study was used to evaluate the skeletal phenotype of the MGP and Twsg1-knockout mouse models to better understand the relationship of osteoporosis, BMP signaling, and mineral metabolism.

TABLE OF CONTENTS

LIST OF TABLES

LIST OF FIGURES

INTRODUCTION

Basic Concepts in Skeletal Biology

There are two different kinds of bone in the human body: flat bones, formed by intramembranous ossification, and long bones that are formed by endochondral ossification. Within the long bones there are two types of bone: spongy/trabecular cancellous bone and cortical/compact bone. Each kind of bone has different functions: trabecular bone, found in the metaphysis and calvaria, is mainly metabolic [1] whereas cortical bone, found in the shaft (diaphysis), is mechanical and protective.[2]

Osteoblasts: Differentiation, Regulation, and Function

There are two main bone cells each having unique functions and properties, the osteoblast (OB) and the osteoclast (OC). The osteoblast is the bone-matrix producing cell and the osteoclast is responsible for resorbing old bone. Osteoblasts originate from a mesenchymal stem cell (MSC) that arises from the mesodermal germ cell layer. The MSC lineage also differentiates into adipocyte, muscle, or chondrocyte lineage. The progression of cells through the proliferation and differentiation stages is tightly regulated by signaling networks which involve transcription factors, co-repressors, and activators. Runx2 and Osterix are the two main transcription factors that push the cells toward the osteoblast lineage. The MyoD family induces the proliferation of MSC into myoblasts, Sox 5,6 and 9 to chondrocytes, while PPAR*y* pushes MSC towards the adipoctye lineage [3]. There are distinct phases of osteoblast differentiation that induce proliferation (pre-osteoblast), matrix maturation (ostoblast), and mineralization

(osteoblast/osteocyte). The osteoblast cell changes its phenotype as it matures and secretes extracellular matrix, which ultimately becomes mineralized [4].

Early pre-osteoblasts are induced by bone morphogenetic proteins (BMPs) -2 and -4 and rapidly proliferate. Other growth factors that induce osteogenesis include: fibroblast growth factors (FGFs), platelet-derived growth factor (PDGF) and transforming growth factor beta (TGF-β) [5]. Pre-osteoblasts express markers such as Type I Collagen, TGF-β, c-Fos/c-Jun, and Twist. Upon commitment to become osteoblasts, the cells stop proliferating and begin to differentiate. Markers of this matrix maturation phase include: Type 1 Collagen, Runx2, and Dlx5 [6]. In the final phase, mineralization, osteoblasts produce extracellular matrix (ECM) proteins such as bone sialoprotein (BSP), osteopontin (OPN), and osteocalcin (OCN) [7]. Some osteoblasts become osteoctyes, which are terminally differentiated and become embedded in the matrix that they are producing. Until recently it was thought that osteocytes have little function in the mature skeleton. However, recent findings have shown that osteocytes have important roles in mechanical sensing and response. [8]

Osteoclasts: Differentiation, Regulation, and Function

Osteoclasts (OC) are the only cells that can resorb bone matrix, and are derived from the monocyte/macrophage lineage. There is a carefully regulated cascade of transcriptional factors controlling differentiation of multinuclear mature OC from mononuclear precursors. Early progenitors and mononuclear cells respond to RANKL (receptor activator of NF-kappa B ligand) and M-CSF (macrophage colony stimulating

factor) and are inhibited by osteoprotegrin (OPG). RANKL, M-CSF, and OPG are all secreted by osteoblasts and stromal cells. Other osteoclastogenesis-promoting factors include interferon gamma, granulocyte macrophage colony-stimulating factor (GM-CSF), and Tumor necrosis factor alpha (TNF- α) [9]. Mature multinucleated functional osteoclasts are comprised of several nuclei and show a characteristic morphology containing “ruffled border” and strong tartrate resistant acid phosphatase (TRAP)-positive staining. This ruffled border contains vacuolar H+ ATPase and acidifies the surrounding bone, producing the “clear zone” that allows the osteoclasts to contact the bone [10, 11]. During differentiation from mononuclear to multinuclear cells, the osteoclasts are activated by RANKL and tumor necrosis factor alpha (TNF-α), and are inhibited by OPG. The cytoplasmic-tail of RANK receptor interacts with TNF-associated factor (TRAF) 1,2, 5 and 6 in the cytoplasm, and these interactions influence the JNK and NF-κB pathways [12]. Numerous transcription factors have been shown to play a role in the formation of mature osteoclasts including PU.1, Nfatc1, AP-1, and MITF which are downstream of the kinase signaling cascades [13].

Fusion of cells is a very interesting phenomenon that allows for fertilization, myotube formation, and bone resorption [14]. In osteoclasts this process is regulated (at least in part) by CD44, CD47, ADAM12, MCP-1 CD9, ATPv6, and DC-STAMP (dendrirtic cell-specific seven transmembrane protein) [15, 16]. During osteoclast differentiation in DC-STAMP-deficient mice, although the mononuclear cells express TRAP, no functional multinuclear osteoclasts are formed. RANKL, c-Fos, and Nfatc1 were induced in these cells, which also showed actin ring formation and ruffled borders. The authors and others showed that DC-STAMP is therefore important for fusion of osteoclasts and giant

cells [16]. Limiting or promoting fusion would lead to hypo or hyper reactive osteoclasts, thereby creating an imbalance in osteoclasts/osteoblasts leading to defective bone production. Other mechanisms such as inflammation, apoptosis, enhanced stem cell/precursor population, and/or accelerated maturation of one cell type could also alter bone remodeling leading to a pathological state [17]. Osteoblasts can promote the formation of osteoclasts by producing RANKL, but can also inhibit by producing the decoy ligand OPG, which competitively binds RANKL and prevents the activation of osteoclasts. This is probably the main mechanism by which osteoclast differentiation is regulated [18].

Extracellular Matrix: Role in Bone and Mineralization

To maintain bone structure there must be a tightly regulated balance between mineral deposition and resorption in the proper location of the body [19]. The extracellular matrix (ECM) is involved in this regulation of mineralization and is comprised of proteins, proteoglycans, and mineral deposits. Mineralized ECM is designed to provide support and resist compression [20]. Physiological mineralization is a cell-mediated process that occurs with contributions from both osteoblasts and chondrocytes. Extracellular matrix mineralization (ECMM) is regulated by 1) MGP (Matrix Gla Protein) 2) Ank 3) NPPS 4) pyrophosphate, and 5) Fetuin [21]. Mineralization in bone and tooth occur in ECM vesicles that along with other components also contain calcium and phosphate ions. Ectopic pathological mineralization is a disease state in which mineral disposition occurs in soft tissue [22]. Mice deficient in MGP show ectopic mineralization of blood vessels suggesting the significance of MGP in regulation of physiological ECMM [23].

Structure, Function and Regulation of Matrix Gla Protein (MGP)

MGP is a 14 kDa secreted ECM protein that is an inhibitor of mineralization. The MGP gene is located on chromosome 12p, is 3.9kb, and contains 4 exons [24]. MGP is a member of the mineral binding family which includes coagulation factors prothrombin, factor VII, factor IX, factor X, protein C, protein S and protein Z [25]. Human MGP has nine glutamate residues and murine MGP has four glutamate residues. Along with these glutamate residues MGP has one disulfide bond and multiple phosphoserine residues. To be fully functional, MGP must undergo two post-translational modifications: the production of gamma-glutamate (GLA) residues and serine phosphorylation. Vitamin K is a cofactor for the post-translational modification of glutamate residues. If these residues are not modified properly (no gamma glutamate present) there is a risk of osteoporosis and vascular calcification in human patients undergoing anticoagulant therapy [28]. It is hypothesized that the GLA residues allow MGP to bind to calcium, resulting in inhibition of mineralization [25, 26]. It is well established that MGP is a developmentally regulated inhibitor of cartilage mineralization that controls mineral quantity [22, 27].

MGP protein localization has been controversial. However, *in vitro* studies have localized Mgp mRNA to osteoblasts, vascular smooth muscular cells (VSMC), calvaria, chondrocytes, kidney, and lung using *in situ* hybridization techniques [29-32]. MGP protein was localized to the skeletal and vascular systems in the marine fish *Prionace glauca* using immunohistochemistry techniques (IHC) [32]. In zebra MGP protein was expressed in ECM (bone), cartilage, and cementum [33]. The current study seeks to better understand the influence of MGP on skeletal tissue, specifically bone.

Phenotype of the MGP Deficient Mouse

MGP-deficient mice have been well characterized and show respiratory, cartilage and vascular smooth muscle cell defects [34]. They die by 2 months of age due to rupture and subsequent hemorrhage of the thoracic and abdominal aorta. The $MGP^{-/-}$ mice exhibit extensive calcification of elastic fibers and collagen fibrils in the media of the aortic wall. This calcification originates at several points and involves all elastic and muscular arteries, but not arterioles, capillaries, or veins. There is no appearance of atherosclerotic plaques in this tissue, and the myocardium appears to be spared. The aortic smooth muscles also show a defect in spatial arrangements and do not form the proper layers in the vessel wall [35].

MGP-deficient mice show an increased heart rate beginning at 2 weeks of age in homozygotes as well as a shortened stature. The differences become more apparent as the animals get older, until death, at which time homozygotes are noticeably smaller than wild-type littermates. In addition, the growth rate peaks at 2-3 weeks of age, but gradually slows down thereafter and the homozygotes exhibit postnatal growth retardation [34]. An osteopenic phenotype was also noted, along with decreased bone density and increased incidence of fracture. However, this reduction in bone was attributed to improper growth plate formation [36]. The mice had skeletal phenotypes beyond the bone phenotype evaluated in this study including abnormal long bone epiphyseal plate morphology [34]. At 8 weeks the homozygotes displayed accelerated calcification of the growth-plate cartilage. This calcification of the growth plate abnormally extends into the zone of proliferating chondrocytes. The mice also exhibited an abnormal long bone epiphyseal plate proliferative zone, a decreased or absent

hypertrophic zone due to abnormal calcification of the growth plate [34, 36]. The columnar appearance of the proliferating zone was not seen, and the cells were very disorganized. Cartilage morphology was not only disrupted in the bone but also in the trachea where the lower end of the trachea was calcified prematurely. The respiratory system also revealed defects including abnormal bronchus morphology in which the mice display inappropriate calcification of cartilage in the main bronchi, and abnormal tracheal cartilage morphology [34].

Despite several publications there is little understanding of the effect of MGP on the differentiation and function of osteoblasts and osteoclasts, and whether osteoblast and/or osteoclasts contribute to the reduced bone density noted in $MGP^{-/-}$ mice. Signaling mechanisms that underlie the osteopenic phenotype in MGP-deficient animals remains unclear.

Twisted Gastrulation

Twisted gastrulation (Tsg, Twsg1) is an extracellular glycoprotein expressed by various cells, including osteoblasts, that plays a key role in regulating BMP function [37]. The protein was originally described in *Drosophila* and contains two evolutionarily conserved cysteine-rich domains (CR) [38]. Twsg1 mRNA gene products have been identified in *Drosophila*, human, mouse, *Xenopus*, zebrafish and chick. Twsg1 plays a role in craniofacial, skeletal, and salivary gland development [39-42], and influences dorsal/ventral embryonic axis patterning by influencing morphogen gradients in the early embryo [43]. BMP ligand and receptor interaction is mediated by Twsg1 and Chordin

(Chd), another secreted BMP antagonist in addition to Noggin, Gremlin, Cerberus, and Follistatin [37]. In the extracellular space a tertiary complex is formed form Twsg1, Chd and BMP ligand. This prevents BMP2 from binding to the receptor thereby blocking SMAD 1/5/8 signaling [37]. It is essential to understand this interaction as BMPs are being used in orthopedic practice to induce spinal fusion, and possibly fracture repair, periodontal regeneration, and prevention of bone loss [44]. Only recently, there have been studies initiated to evaluate the role of Twsg1 in mammalian skeletal and embryonic development [40, 41, 45, 46]. Twsg1 acts as both an agonist and antagonist of BMP signaling. Acting as an antagonist, Twsg1 promotes the formation of stable tertiary BMP/Chordin/Twsg1 complexes, which prevent binding of BMPs to their cell surface receptors [47-51]. Second, when acting as an agonist of BMP signaling, the stability of the inhibitory tertiary complex (BMP+ Chordin+ Twisted Gastrulation) is controlled by the BMP-1/Tolloid metalloprotease enzyme, which cleaves Chordin at specific sites [47-49, 52]. In the presence of Twsg1, Chordin is a better substrate for cleavage by the BMP-1/Tolloid enzyme [50, 51]. By promoting Chordin degradation in the presence of BMP-1/Tolloid, Twsg1 releases BMP that is now able to signal through BMP receptors, thereby behaving as a BMP agonist [53]. This cleavage of Chordin by the BMP-1/tolloid enzyme is the switch between the opposing functions of Twsg1.

Generation of Twsg1 Deficient Mouse and Phenotypes

Twsg1-null (Twsg1 $^{-/-}$) mice were produced by deleting the BMP2 binding domain present in exon 3 in two different pure backgrounds: C57BL/6 and 129Sv/Ev. Twsg1$^{-/-}$ C57BL/6 mice have severe craniofacial defects and die in the prenatal period, precluding the study of the postnatal bone formation [40]. These mice exhibit forebrain defects

including rostral truncations, holoprosencephaly, cyclopia, as well as alterations in the first branchial arch leading to lack of jaw (agnathia). Zakin and De Robertis observed a similar phenotype in Twsg1$^{-/-}$ mice only when crossed with BMP4$^{+/-}$ mutants, indicating that Twsg1 interacts genetically with BMP4 [41]. Twsg1$^{-/-}$ mice in the pure 129Sv/Ev background, which were used in my studies, are viable and fertile but small in stature.

PROJECT SUMMARY

Characterize the *in vivo* skeletal phenotypes in the MGP and Twsg1 deficient mice and understand the effect of MGP-deficiency on osteoblast and osteoclast differentiation and function.

Aims of the Study

The **first aim** of the study was to characterize the *in vivo* skeletal phenotype of the Twsg1$^{-/-}$ mouse using both static and dynamic histomorphometric analysis. Static measurements utilized μCt and histology preparations. Analysis was performed on 3 month old wild-type mice (WT) and Twsg1$^{-/-}$, and dynamic histomorphometric analysis

using tetracycline dye to evaluate the bone formation rate in 1-3-6 month old WT and Twsg1$^{-/-}$ mice.

The **second aim** evaluated the *in vivo* skeletal phenotype of the MPG$^{-/-}$ using static histomorphometric analysis on femurs of 2 and 4 week old mice, and determined the status of osteoblast and osteoclast differentiation in MGP$^{-/-}$ mice.

MATERIALS AND METHODS

Generation and Maintenance of the Twsg1 Colony and Genotyping

Animals were created by Dr Anna Petryk as previously described [40, 47]. Twsg1 heterozygous (Twsg1$^{+/-}$) 129Sv/Ev mice were bred to obtain WT and Twsg1$^{-/-}$ mice. Genotyping was performed as previously described [54]. The conditions used for genotyping were 94^{0}C for 3 min, 94^{0}C for 30sec, 58^{0}C for 40sec, 72^{0}C for 1min, repeat for 39 cycles followed by 72^{0}C for 7 min. Primer sequences used for genotyping can be found in Table 3.

Maintenance of MGP mouse Colony and Genotyping

$MGP^{+/-}$ C57Bl/6 animals were obtained from the laboratory of Gerard Karsenty, (Columbia University). Breeding pairs were maintained using $MGG^{+/-}$ males and females, confirmed by genotype. Primers can be found in Table 3. The PCR conditions used for genotyping were 94^0C for 3 min, 94^0C for 30sec, 58^0C for 40sec, 72^0C for 1min, repeat for 39 cycles followed by 72^0C for 7 min.

Digital Photos and Faxitron Analysis

Whole animal digital photos were taken using an Olympus Eclipse scope and CoolPix990 digital camera. X-rays were taken of the femur and tibia upon dissection using a Specimen Radiography System Model MX-20 (Faxitron X-ray).

MicroCt Analysis

Micro CT analysis of femurs was performed at the Physiological Imaging Center, Rochester, MN. The bones were reconstructed and static parameters were measured using Amira 4, Analyze 6, Matlab, Image J, and Photoshop. Parameters measured include cortical thickness (mm), which is a direct measurement of mid-diaphysis cortical thickness, and bone diameter, which measures the total distance across the cortical bone and marrow of the same region. Trabecular measurements include separation, thickness, and number present on the distil end of the femur viewed in the middle of the bone on a longitudinal plane. Trabecular thickness is a measurement of the average trabecular thickness at the widest point of all trabeculae in the represented bone slice. Trabecular number is the average of all the trabeculae present in one femur. Trabecular spacing measures the average surface-to-surface trabecular separation at the closest

point within the distil femur. Tissue volume is a 3D measurement which takes into account all the marrow space and all the bone present within articular cartilage with the material subtracted above the growth plate. Total bone volume represents the volume of cortical bone added to the volume of trabecular volume. Tissue and total bone volume parameters take into account the entire bone minus the area above the growth plate. Cortical area is a 2D measurement that contains only the shaft of the bone with the trabeculae removed.

Dynamic Histomorphometric Measurement of Twsg1 Wild type and Deficient Mice

Animals were injected with tetracycline dye (25mg/kg) 5 days apart and sacrificed 2 days after the last injection. Image J and Photoshop were used to determine the mineral apposition rate (MAR) in 1-3-6 month old WT and Twsg1$^{-/-}$ mice.

Primary Osteoblast Culture

Primary osteoblasts were isolated as previously described [54]. Calvaria from 7- to 10-day-old WT or knockout mice were dissected and subjected to sequential digestions with 2 mg/ml of collagenase A in MEM solution containing 0.25% trypsin for 20, 40, and 90 min. The third digestion was plated at 1.5 x10^4 cells/cm^2. Cells were maintained at 37°C in a humidified atmosphere of 5% CO_2, in MEM media containing 10% FBS, 1% penicillin/streptomycin, and 1% nonessential amino acids. On reaching confluency, cells were differentiated with ascorbic acid (50ug/ml)–containing media.

Primary Osteoclast Cultures

Osteoclasts were obtained as previously described [55] from bone and spleen cells. Spleens were mechanically dissociated or bone marrow flushed from femurs. Resulting cells were cultured for 3 days in the presence of 50 ng/mL M-CSF on non–tissue culture dishes. The adherent cell population, containing the committed osteoclast precursors, was cultured for the indicated amount of time with M-CSF (50 ng/mL) and 60 ng/mL RANL to induce differentiation. This work was performed in collaboration with Julio Sotillo.

RNA Isolation

Status of cellular differentiation was assessed by real-time RT-PCR. Total RNA was isolated from cells using TRIzol reagent and quantitated by UV spectroscopy. RT was performed using 1ug of RNA and the iScript cDNA Synthesis kit.

Real Time Quantitative PCR

Quantitative real-time RT-PCR of osteoblast and osteoclast genes was performed using a Mx3000P QPCR System for osteoblast analysis and MyiQ Single-Color Real-Time PCR Detection System (Bio-Rad) for osteoclast analysis. This analysis was performed using 1 μl of the cDNA with 13 Brilliant SYBR Green master mix (osteoblast) or 23 iQ SYBR Green supermix (osteoclast). Osteoblast genes were normalized to GAPDH mRNA, and osteoclast genes were normalized to L4 mRNA. Primer sequences for all

genes analyzed are provided in Table 3. The sequences were designed using Primer 3 [56] or obtained from previous publications [57].

Osteoblast Differentiation

Calvarial-derived osteoblast cells were plated at 25.000 cells/cm^2 and were treated with ascorbic acid (50 ug/ml) upon reaching confluence. Cells were allowed to differentiate for 8 and 16 days.

Alkaline Phosphatase Assay

Primary calvarial-derived osteoblasts were washed in 1x PBS and harvested for alkaline phosphatase activity in buffer containing 0.2mM Tris and 0.004% NP-40. Following sonication the cell lysate was exposed to the substrate p-nitrophenylphosphate and colorimetric readings were taken.

Mineralization Assay

Mineralization of primary cells was evaluated by Von Kossa staining as previously described [37]. Briefly, cells were fixed in 95% alcohol for 15 minutes at 37°C. The plates were stained with 5% $AgNO_3$ for 1 hour at 37°C. Following washing with water, the plates were exposed to bright light overnight and evaluated for staining.

Osteoblast Gene Expression

Quantitative real-time RT-PCR of osteoblast and osteoclast genes (Bone sialoprotein and osteocalcin) was performed using a Mx3000P QPCR System (Stratagene) This analysis was performed using 1 μl of the cDNA with 12μl Brilliant SYBR Green master mix which includes ROX reference dye. Osteoblast genes were normalized to GAPDH mRNA. The data represented is the fold change between control and ascorbic acid treated cells. Genes are listed in Table 3.

Osteoclast Differentiation Studies

Bone marrow and spleen-derived osteoclasts were plated in MEM containing M-CSF (10 ng/mL) and 60 ng/mL RANKL and allowed to differentiate for 5-7 days. The media was changed every other day.

Histomorphometry of Osteoclast Number and Size

For *in vivo* evaluation femurs of 1 month old WT and $Twsg^{-/-}$ mice were fixed in 10% neutral buffered formalin and embedded in paraffin. Sections of 5 micron thickness were made using a microtome. Samples were TRAP stained using Acid Phosphatase, Leukocyte (TRAP) Kit. Bone marrow cultures were used for *in vitro* analysis and TRAP stained after 7 days in RANKL containing media. Representative images were taken randomly using a Nikon CoolPix 990 digital camera. Image J was used to evaluate the number and size of osteoblasts.

Osteoclast Gene Expression

Quantitative real-time RT-PCR of osteoclast genes TRAP and DC-STAMP was performed using the iQ Single-Color Real-Time PCR Detection System. This analysis was performed using 1μl of cDNA and 23ul iQ SYBR Green supermix (Bio-Rad, respectively). Osteoclast genes were normalized to L4 mRNA. Primer sequences for all genes analyzed are provided in Table 3. The sequences were designed using Primer 3 [56] or obtained from previous publications [57].

Evaluation of Serum Bone Markers in MGP$^{-/-}$ Mice

Blood was collected from WT and MGP-deficient mice and used to determine serum levels of OPG and CTX by ELISA (OPG: Alpco, CTX: RatLaps™ Immunodiagnostics Systems).

Statistical Analysis

All statistical analysis was performed using Prism 4 (Graphpad Software, Inc., San Diego, CA). Real-time RT-PCR analysis is reported as mean ±SD of duplicate independent samples from at least two independent RNA experiments. ANOVA and Student's t-test were used to assess significance between groups.

DATA AND RESULTS

The **first aim** of the study was to characterize the *in vivo* skeletal phenotype of the Twsg1$^{-/-}$ mouse using both static and dynamic histomorphometric analysis. Static measurements utilized μCt and histology preparations. Analysis was performed on 3 month old wild-type mice (WT) and Twsg1$^{-/-}$, and dynamic histomorphometric analysis using tetracycline dye to evaluate the bone formation rate in 1-3-6 month old WT and Twsg1$^{-/-}$ mice.

Twsg1$^{-/-}$ mice were smaller in size compared to WT littermates (Figure 1A). These mice also showed reduced bone density using X-ray as seen in femurs from 1 month old animals (Figure 1B). Femurs from WT and Twsg1$^{-/-}$ mice were evaluated using μCt technology and found to have significantly reduced bone volume as compared to WT controls. A 3D image representing the femur of 3 month old WT and Twsg1$^{-/-}$ mouse can be seen in Figure 1C. An isoslice of both a cross-sectional image of the shaft and longitudinal image of the distil image of the femur can be seen in Figure 1D, this image

represents the cortical and trabecular bone. Quantification of 3 month WT and Twsg1-deficient mice using common static bone parameters can be seen in Figure 2 and Table 1. The most striking differences can be seen in the reduction of cortical area, cortical volume, and trabecular separation in the Twsg1-deficient mice ($P < 0.001$).

Mineral apposition rate (MAR) was measured at 1, 3, 6 month old mice to determine if osteopenic phenotype was due to changes in osteoblast function. A representative image (Figure 3A) shows cortical bone of the femur. As shown in Figure 3B and 3C there is no significant change in MAR between WT and Twsg1$^{-/-}$ per day. This data indicates that the osteopenia in Twsg1$^{-/-}$ mice is most likely not due to a defect in osteoblast function.

The **second aim** evaluated the *in vivo* skeletal phenotype of MPG$^{-/-}$ using static histomorphometric analysis on femurs of 2 and 4 week old mice, and determined the status of osteoblast and osteoclast differentiation in MGP$^{-/-}$ mice

To understand the mechanism for the osteopenic phenotype in MGP$^{-/-}$ mice, micro computer tomography (μCt) was utilized to quantify histomorphometric measurements of MGP-deficient mice compared to WT. Analysis was performed on WT and MGP$^{-/-}$ mice at 2 -and 4 week time points. As shown in Figure 4, the MGP-deficient mice exhibited osteopenia in long bones when examined by x-ray (Figure 4B) and μCT (Figure 4A). The distal portion of the femur is illustrated in 4A with both longitudinal (top) and cortical images (bottom). The heterozygous animals had a phenotype essentially identical to the WT animal when examined by X-ray (data not shown) and therefore the histomorphometric measurements were performed on only MGP$^{-/-}$ and WT animals. An

outline of the bone parameters evaluated in both mouse lines is shown in Table 4, the results of MGP histomorphometry is shown in Table 2 and Figure 5.

Our results show a significant reduction in cortical volume between WT and $MGP^{-/-}$ (14.265 mm^3 $MGP^{+/+}$ vs. 5.07mm^3 $MGP^{-/-}$ 4 week old animals, $P < 0.05$). Total bone volume was significantly reduced in the $MGP^{-/-}$ animals at both 2 and 4 week age groups (12.15mm3 $MGP^{+/+}$ vs. 7.52mm^3 $MGP^{-/-}$ 2 weeks, and 25.16mm^3 $MGP^{+/+}$ vs. 14.88mm^3 $MGP^{-/-}$ 4 weeks, $P< 0.05$). The bone diameter showed a significant reduction at 4 weeks of age (1.45mm $MGP^{+/+}$ vs. 1.2mm $MGP^{-/-}$, $P < 0.05$).

There was no difference in trabecular thickness between the genotypes at 2 week age group. Similarly, only a slight difference, which was not significant, was observed in trabecular thickness for the 4 week age group (0.167mm $MGP^{+/+}$ vs. 0.045mm $MGP^{-/-}$ NS). Trabecular separation was increased although not significantly in the $MGP^{-/-}$ at 4 weeks only (0.11mm $MGP^{+/+}$ vs. 0.805mm $MGP^{-/-}$, NS). The WT animals had twice as many trabeculae at 4 weeks as the $MGP^{-/-}$ mouse (20 $MGP^{+/+}$ vs. 10 $MGP^{-/-}$, $P<0.05$). Cortical Volume/Tissue Volume showed a slight but non-significant reduction in the MGP-deficient animals at 2 weeks, where as this parameter was significantly reduced in the 4 week old $MGP^{-/-}$ mice compared to WT mice (0.429 mm^3 $MGP^{+/+}$ vs. 0.277 mm^3 $MGP^{-/-}$, $P < 0.05$). Cortical Volume/Total Bone Volume was lower, but not significantly, at both time points (0.317mm^3 $MGP^{+/+}$ vs. 0.276 mm^3 $MGP^{-/-}$, at two weeks and 0.566mm^3 $MGP^{+/+}$ vs. 0.349mm^3 $MGP^{-/-}$ at four weeks). Our data clearly demonstrates disruption of both the cortical and trabecular bone in the $MGP^{-/-}$ mice. We next sought to determine if

the osteopenic phenotype in the MGP$^{-/-}$ was due to a defect in either osteoblast or osteoclast differentiation and function.

Osteoblast differentiation is accelerated in primary osteoblasts from MGP$^{-/-}$ mice

To determine whether a defect in osteoblast function is responsible for the osteopenic phenotype, primary calvarial cells were obtained from 5-9 day old pups. The cells were differentiated for 2, 4 or 7- weeks, following which the ability of the cells to mineralize was measured. Primary osteoblasts from MGP$^{-/-}$ mice show premature mineralization after two weeks in Ascorbic Acid and Betaglycerol phosphate containing medium where as the WT cells underwent mineralization at 4 weeks of age (Figure 6A).

MGP-deficiency leads to elevated OCN and BSP mRNA levels compared to WT mice at 8 and 16 days

We next evaluated expression of bone sialoprotein (BSP) and osteocalcin (OCN), key osteoblast differentiation genes, to determine if accelerated mineralization of MGP$^{-/-}$ osteoblast cultures could be explained by enhanced differentiation using real time RT-PCR. Figure 6B shows that there is a significant increase in BSP mRNA at both the 8 and 16 day time points, with a greater increase on day 8. OCN (Figure 6C) mRNA levels were also elevated at both time points, however the 8 day time-point was not significant. There was a significant elevation in OCN at the 16 day time point ($p < 0.001$).

MGP$^{-/-}$ osteoblasts have elevated levels of alkaline phosphatase at 8 and 16 days compared to WT

Alkaline phosphatase (ALP) activity was compared in primary osteoblasts obtained from both WT and MGP$^{-/-}$ mice. MGP deficiency resulted in enhanced ALP activity at both 8 and 16 day time points as shown in Figure 6D.

It is not clear why MGP$^{-/-}$ bones that show an osteopenic penotype also show enhancement of ALP activity, accelerated mineralization, and increased levels of osteoblast gene expression. One reason is that the osteoblasts rapidly differentiate and mature followed by apoptosis. Therefore they are not long lived and do not add significant bone mass. The accelerated mineralization can be explained in part by early differentiation of MGP$^{-/-}$ cells. Another explanation for an osteopenic phenotype with accelerated mineralization and osteoblast differentiation is a concomitant increase in bone resporption that exceeds bone formation. The status of osteoclast differentiation was next investigated.

Mgp$^{-/-}$ mice show increased TRAP activity compared to WT mice

To determine if osteoclasts played a role in the osteopenic phenotype, various measures of osteoclast differentiation and bone resorption were evaluated using bone sections, and both spleen and bone marrow derived primary osteoclasts.

As shown in Figure 7A, histological sections of femurs from WT and MGP$^{-/-}$ mice showed an increase in both number and size of TRAP positive multinucleated osteoclasts. Similarly, *in vitro* osteoclast cultures from Mgp$^{-/-}$ mice showed an increase in the number and size of TRAP+ multinucleated osteoclasts relative to WT mice (Figure 7B). Quantification of osteoclast size and number (Figure 7 C, D) illustrated an enhancement in both measurements in MGP-deficient mice ($P > 0.05$). To evaluate whether increased size of TRAP positive multinucleated osteoclasts is due to premature fusion of MGP$^{-/-}$ mice, we performed a time course experiment comparing when fusion occurred in MGP$^{-/-}$ osteoclasts compared to WT mice. During culture, fusion occurred 24-hours earlier in the MGP-deficient osteoclasts then in wild-type osteoclasts (Figure 7E).

Evaluation of DCSTAMP and TRAP mRNA in Mgp$^{-/-}$ osteoclasts compared to WT

Next we evaluated the expression of osteoclast genes from WT and MGP $^{-/-}$ mice during osteoclast differentiation. First we evaluated osteoclasts endogenously express MGP mRNA, and whether this expression changes with RANKL exposure. It can be seen in Figure 8A that wild type cells express MGP, and this expression does not change with exposure to RANKL or stage of differentiation from pre-osteoclast to multinucleated osteoclasts. mRNA from primary calvarial-derived osteoblast cells were used as controls. This data shows that MGP is endogenously expressed and may have an intrinsic role in the regulation of bone resorption.

To better understand possible molecular mechanisms behind the large multinuclear osteoclasts, both TRAP and DC-STAMP mRNA were evaluated after 5 days in culture (±60 ng/ml RANKL). TRAP mRNA levels were significantly elevated in MGP$^{-/-}$ (Figure

8B, P< 0.05) compared to wild type cells. DC-STAMP showed an even more significant enhancement in MGP-deficient cells (Figure 8C, P< 0.0001). These experiments show osteoclastogenesis is significantly altered in $MGP^{-/-}$ mice

OPG/RANKL Levels in $MGP^{-/-}$ mice remained unchanged

Next, to evaluate whether changes in RANKL/OPG levels in $MGP^{-/-}$ mice are a possible cause for increased osteoclastogenesis, RANKL and OPG levels were evaluated in WT and $MGP^{-/-}$ mice. Serum OPG levels were not significantly different in WT and $MGP^{-/-}$ as measured by ELISA (Figure 9A, NS). We also evaluated mRNA expression of RANKL and OPG in WT and $MGP^{-/-}$ primary calvarial osteoblasts using real time RT-PCR. As shown in Figure 9B, RANKL and OPG mRNA expression was not significantly different in $MGP^{-/-}$ compared to WT osteoblasts. These findings suggest that enhanced osteoclastogensis is a result of intrinsic changes in the osteoclast rather then through contributions from osteoblasts.

Enhanced resorption in $Mgp^{-/-}$ osteoclasts

Next we evaluated whether enhanced osteoclastogenesis observed in $MGP^{-/-}$ was associated with enhanced resorption. As shown in Figure 9C, serum CTX levels were significantly elevated in $MGP^{-/-}$ mice compared to WT mice as determined by ELISA (P< 0.05). These results demonstrated that the absence of MGP causes a physiological change in the animals with an enhancement of osteoclast differentiation leading to osteoclasts that are both larger in size and greater in number, as well as activity.

Measurement of calcium, phosphorus, and parathyroid hormone in MGP$^{-/-}$

There are two possibilities that may explain this enhanced osteoclastogenesis in MGP$^{-/-}$ mice. The first is that MGP-deficiency causes a direct effect on osteoclasts leading to enhanced osteoclastogenesis. The excess calcium released from bone will cause hypercalcemia resulting in ectopic mineralization throughout the vascular system (as observed in MGP$^{-/-}$). There would be no global changes in PTH or phosphate in this situation.

The second possibility for enhanced osteoclastogensis, we propose, is due to secondary hyperparathyroidism (SHPT) that results from an indirect mechanism. We propose that vascular calcification in MGP$^{-/-}$ mice causes hypocalcemia, thereby causing secondary hyperparathyroidism (SHPT) which activates osteoclasts and increases bone resorption. The signs of SHPT include retention of phosphorus (hypophosphatemia), decrease in serum calcium (hypocalcemia), decreased vitamin D metabolism, and increase in serum PTH levels (hyperparathyroidism). We therefore evaluated the status of serum calcium, phosphorus and PTH in Mgp$^{-/-}$ mice compared to WT mice. These experiments were performed in collaboration with Dr Monsur Murshed. As shown in Figure 9 serum calcium levels (D), inorganic phosphate levels (E), PTH levels (F) showed no significant changes in Mgp$^{-/-}$ mice compared to WT animals. These results show that the enhanced osteoclastogenesis is an intrinsic mechanism due to some change inherent to the

osteoclast and not due to SHPT in these mice or global fluctuations in serum mineral concentrations.

Hypothesis 1: Osteopenia occurs prior to aortic calcification

1. Lack of MGP protein leads to increased osteoclastogenesis
2. Release of calcium which moves to the aorta, leading to pathologic mineralization

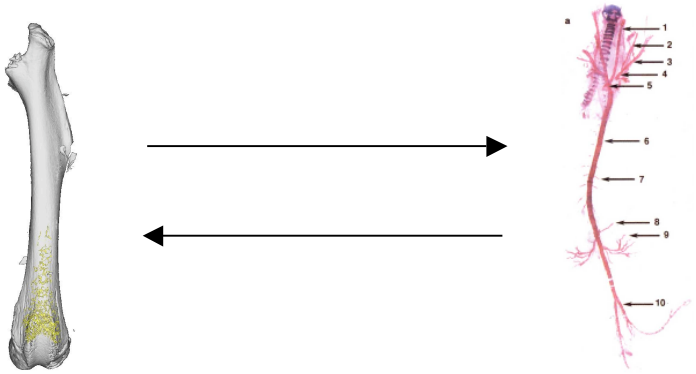

Hypothesis 2: Bone phenotype secondary to SHPT

1. Aorta becomes calcified removing calcium from general circulation
2. Parathyroid gland senses drop in serum calcium (SHPT)
3. Secretion of PTH, activation of osteoclasts via osteoblasts
4. Bones become osteopenic

In summary, our results illustrate osteopenia in $MGP^{-/-}$ mice along with premature osteoblast mineralization and enhanced osteoblast differentiation. Further, $MGP^{-/-}$ mice show hyperactive osteoclasts and increased bone resorption. $MGP^{-/-}$ mice show increased number and size of TRAP-positive multinuclear osteoclasts with elevated levels of both DCSTAMP and TRAP mRNA. These results show the phenotype is in part due to enhancement of the fusion step from mononuclear to multinuclear cells, and these larger cells also produce more CTX fragments indicating they were functionally

changed. Future studies will focus on determining the signaling pathways regulating fusion and also more detailed study of the molecules responsible for fusion.

CONCLUSIONS

In this study we used μCT technology to characterize the skeletal phenotypes of MGP and Twsg1 deficient mice. Data revealed a striking loss in the amount of bone in both MGP and Twsg1 deficient animals. The $MGP^{-/-}$ mice were further evaluated *in vitro* using osteoblast and osteoclast cultures revealing enhanced osteoclastogenesis as one possible cause of the osteopenic phenotype. An additional explanation of the reduced bone in MGP-deficiency could be accelerated osteoblast differentiation resulting in premature mineralization and increased apoptosis. This would hypothetically reduce the amount of bone-forming osteoblast cells and lead to net bone loss. The $Twsg1^{-/-}$ mouse also showed reduction in both cortical and trabecular bone parameters compared to WT. However, this reduction could not be explained by a change in osteoblast activity since the mineral apposition rate was not altered with the loss of Twsg1. The $Twsg1^{-/-}$ has since been studied in great detail in our laboratory, and the results concluded that the osteopenic phenotype was due to enhanced osteoclastogenesis due to an increase in BMP activity acting directly on the osteoclasts [44, 54].

Skeletal characterization of both $Twsg1^{-/-}$ and $MGP^{-/-}$ mice provide an understanding into the function of both Twsg1 and MGP protein, respectively. Twsg1 study has the potential to be used in clinical therapies as an anti-resorptive. $MGP^{-/-}$ mice are relevant in understanding clinical processes such as regulation of mineral homeostasis,

osteoporosis, and calcification. MGP is a likely candidate to counter ectopic calcification. $MGP^{-/-}$ mice also provide understanding to the molecular events surrounding the relationship between vascular calcification and the loss of bone.

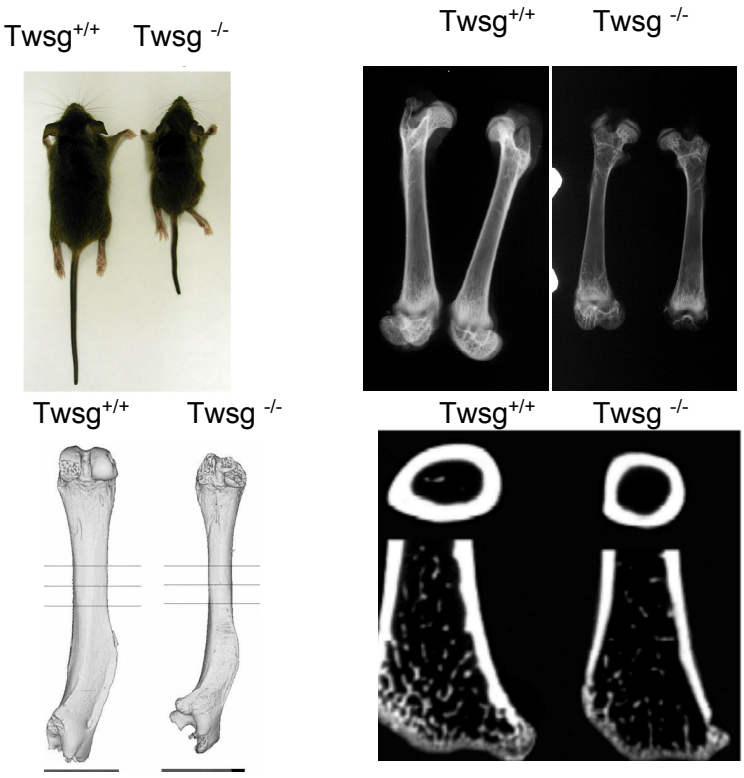

Figure 1 Bone phenotype of Twsg-deficient mouse
In all images: wildtpye (L) and knockout (R)
A) 3month old Wildtype and Twsg $^{-/-}$ siblings
B) Faxitron image of L and R femurs from 1-month old mice
C) Amira rendering of femurs (3 month old animlas)
D) Representation of uCT isoslice: Cross section showing cortical bone (top) and distil femur longitudinal sections illustrating trabecular bone (bottom)

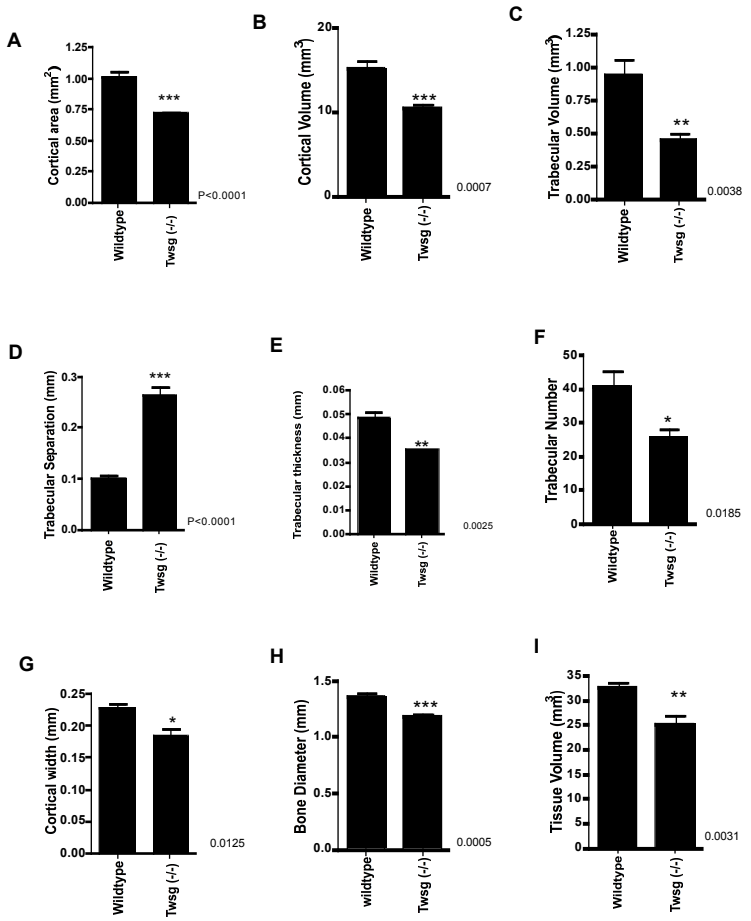

Figure 2: Static Bone Parameters in 3 month old wildtype and Twsg$^{-/-}$ mice show less bone present in Twsg-deficient animals (n=6)
A) Cortical area B) Cortical volume C) Trabecular volume D) Trabecular separation E) Trabecular thickness F) Trabecular number G) Cortical width H) Bone Diameter (mm) I. Tissue volume *p< 0.05; ** p < 0.01; ***p < 0.001

	Twsg1$^{+/+}$	**Twsg1$^{-/-}$**	**P Value**
Bone Diameter (mm)	1.35 ± 0.069	1.1932 ± 0.04	P < 0.01
Tissue Volume (mm^3)	32.681 ± 2.347	24.838 ± 3.59	P < 0.01
Cortical Width (mm^3)	0.223 ± 0.014	0.184 ± 0.033	P < 0.05
Cortical Area (mm^2)	1.105 ± 0.107	0.718 ± 0.04	P< 0.001
Cortical Volume (mm^3)	15.083 ± 1.99	10.390 ± 1.27	P< 0.001
Trabecular Thickness (mm)	0.0432 ± 0.007	0.0349 ± 0.0005	P < 0.01
Trabecular Separataion (mm)	0.101 ± .18	0.2646 ± 0.042	P< 0.001
Trabecular Number	40.566 ± 11.51	25.6 ± 6.14	P < 0.05
Trabecular Volume (mm^3)	0.942 ± 0.30	0.444 ± 0.129	P < 0.01

Table 1: Static histomorphometric analysis of 3 month old wildtype and Twsg-deficient mice (N=6) noting significant changes in all bone parameters in the Twsg $^{-/-}$ mice

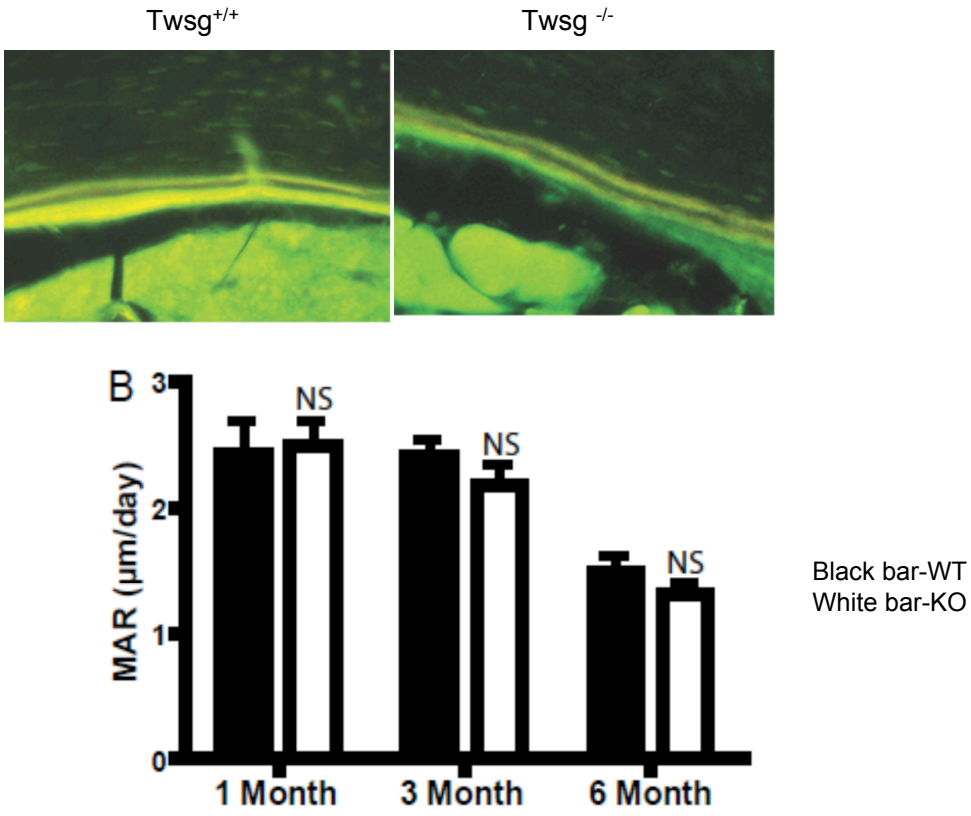

Figure 3: Dynamic Histomorphometric analysis in 1-3-6 month old Wildtype and Twsg $^{-/-}$ mice show no difference in MAR between genotypes. n = min of 3 animals
A. Tetracycline double label (5 days) showing no change in MAR between Wildtype (L) and Twsg$^{-/-}$ (R)
B Graphical representation of mineral apposition rate (MAR) in trabecular bone of femur Black bar-WT White bar- Twsg$^{-/-}$ Data not significant (NS)

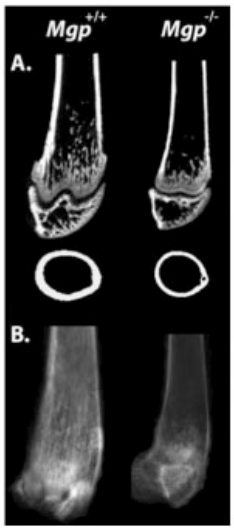

TABLE 2	2 week Mgp WT	2 week Mgp KO	4 week Mgp WT	4 week Mgp KO
Cortical Width (mm)	0.088 ± 0.01	0.065 ± 0.01	0.125 ± 0.01	0.079 ± 0.01 *
Cortical Volume (mm^3)	4.48 ± 1.55	2.08 ± 0.62	14.27 ± 1.61	5.07 ± 3.05 *
Trabecular Thickness (mm)	0.043 ± .006	0.043 ± 0	0.167 ± 0.17	0.045 ± .004
Trabecular Separataion (mm)	0.144 ± 0.09	0.16 ± 0.07	0.11 ± .004	0.805 ± 0.84
Trabecular Number	12.65 ± 3.32	9.45 ± 0.21	20.815 ± 2.14	10.67 ± 0.47 *
Total Bone Volume (mm^3)	12.15 ± 0.47	7.52 ± 1.79	25.16 ± 1.66	14.88 ± 1.13 **
Cortical Volume /Tissue Volume (mm^3)	0.280 ± 0.10	0.181 ± 0.013	0.429 ± 0.027	0.277 ± 0.152 *
Cortical Volume /Total Bone Volume (mm^3)	0.371 ± 0.14	0.276 ± 0.02	0.566 ± 0.03	0.349 ± 0.23
Bone Diameter (mm)	1.17 ± 0.03	1.11 ± 0	1.45 ± 0.03	1.2 ± 0.07 *

Figure 4 Bone phenotype of Wildtype and $Mgp^{-/-}$ animals
A) Micro-CT and X-ray (B) images of 4 week old femurs from $Mgp^{-/-}$ showing reduced bone compared to $Mgp^{+/+}$ mice
Table 2 Cortical and trabecular bone values for static histomorphometric analysis of the femur in 2 and 4 week old animals (n=2) quantify the reduced bone in $Mgp^{-/-}$ animals
*p< 0.05; ** p < 0.01; ***p < 0.00

Figure 5 Static Histomorphometric analysis of 2 and 4 week old wildtype and MGP-deficient mice. A) Cortical width B) Cortical volume C) Trabecular thickenss D) Trabecular separation E) Trabecular number F) Total bone volume G) Cortical bone volume/ total tissue volume H) Cortical bone volume/total bone volume I) Bone diameter *p< 0.05; ** p < 0.01; ***p < 0.001

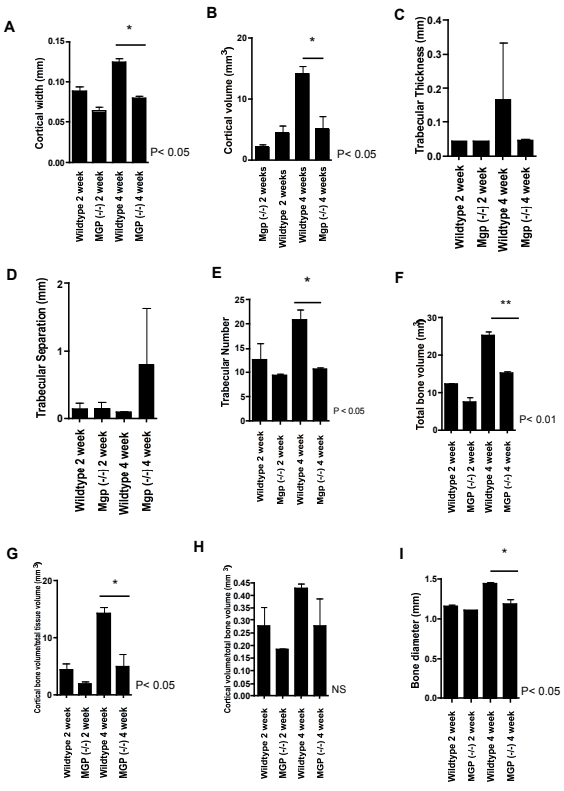

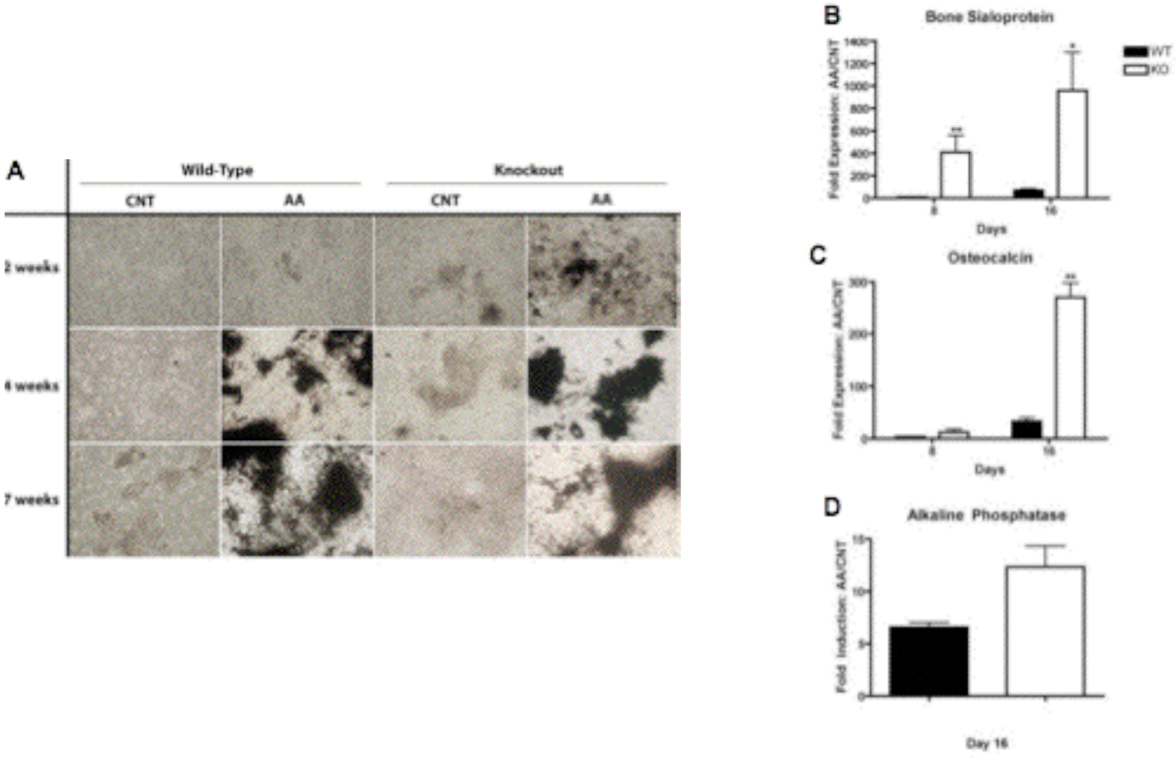

Figure 6 Primary osteoblasts from $Mgp^{-/-}$ mice show premature mineralization and enhanced differentiation

A. $Mgp^{-/-}$ derived osteoblasts show premature mineralization. Calvarial primary osteoblasts were isolated from $Mgp^{+/+}$ and $Mgp^{-/-}$ animals and grown in MEM with β-glycerolphosphate (10 mM) in the absence or presence of ascorbic acid (AA) 50mg/ml.

B) BSP and C) OCN expression is elevated in $Mgp^{-/-}$ mice on both 8 and 16 days

D)Higher ALP is noted in $Mgp^{-/-}$ osteoblasts compared to $Mgp^{+/+}$ osteoblasts

*p< 0.05; ** p < 0.01; ***p < 0.001

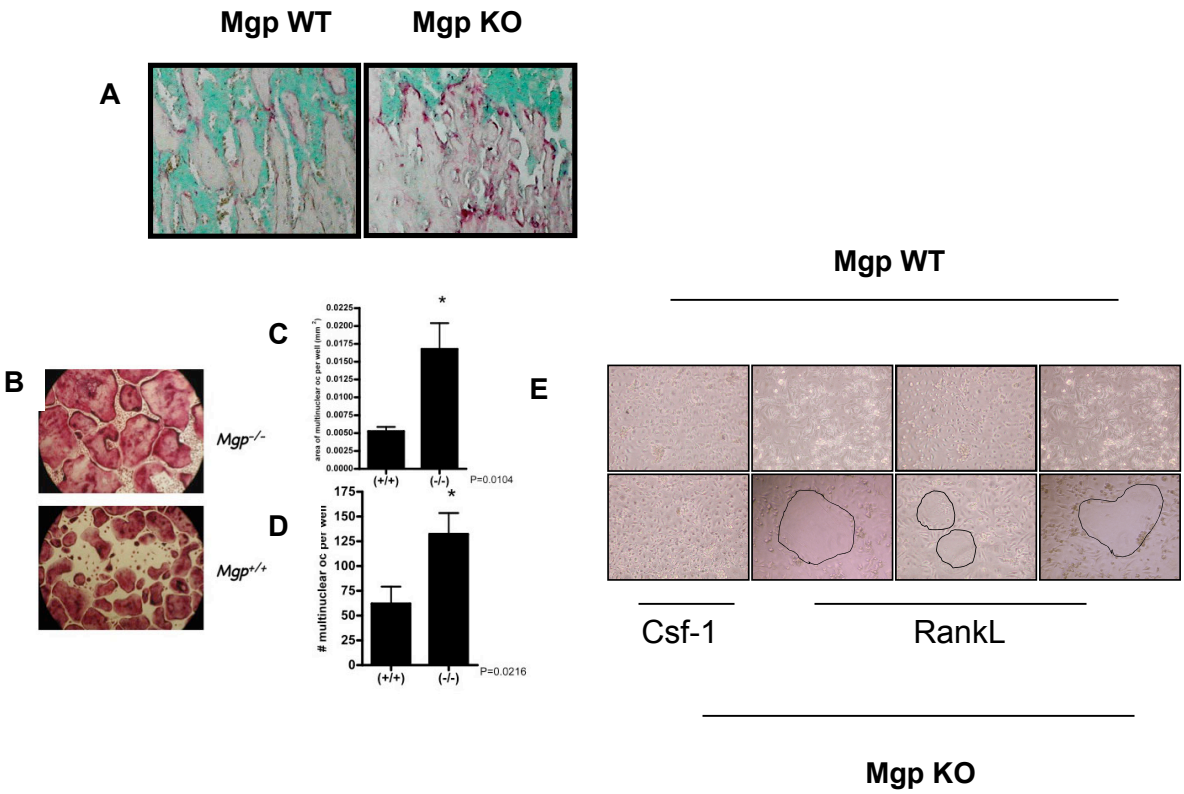

Figure 7 Enhanced osteoclastogenesis in $Mgp^{-/-}$ mice.
A) *In vivo* analysis: Histological sections following TRAP stain of WT (L) and $Mgp^{-/-}$ (R) mice showing intense staining in MGP-deficient bone
B) *In vitro* osteoclasts from bone marrow in WT (L) and $Mgp^{-/-}$ (R) mice
C) Quantification of size of TRAP-postive osteoclasts *in vitro*
D) Quantification of number of TRAP-positive osteoclasts *in vitro*
E) Time course experiment evaluating fusion in CSF ± RANKL cultures from MGP WT and $MGP^{-/-}$

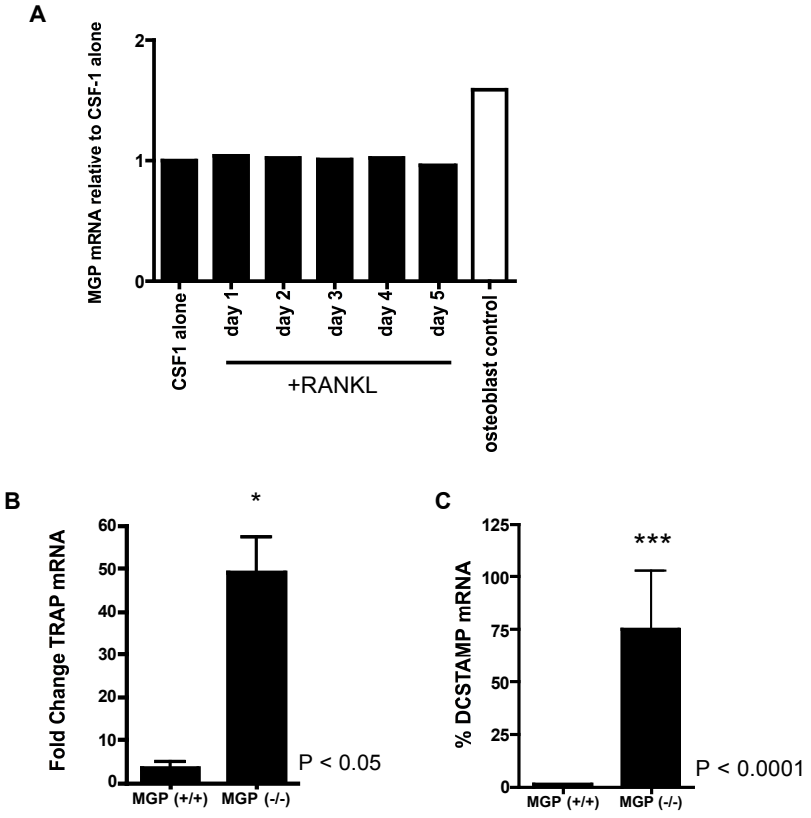

Figure 8 Gene expression levels in MGP osteoclasts
A) Wildtype cells illustrate that MGP mRNA does not change with RANKL treatment and differentiation. Primary calvairial osteoblasts were used as a control. Data is relative to CSF-1 alone. Up regulation of TRAP (B) and DC-STAMP (C) mRNA in $Mgp^{-/-}$ osteoclasts. Realtime PCR analysis in osteoclast cultures (mCSF 10 ng/ml) and RANKL (60 ng/ml) for 5 days. Mean fold mRNA change (RANKL + mCSF/mCSF alone); normalized to L4 gene. *p< 0.05; ** p < 0.01; ***p < 0.001

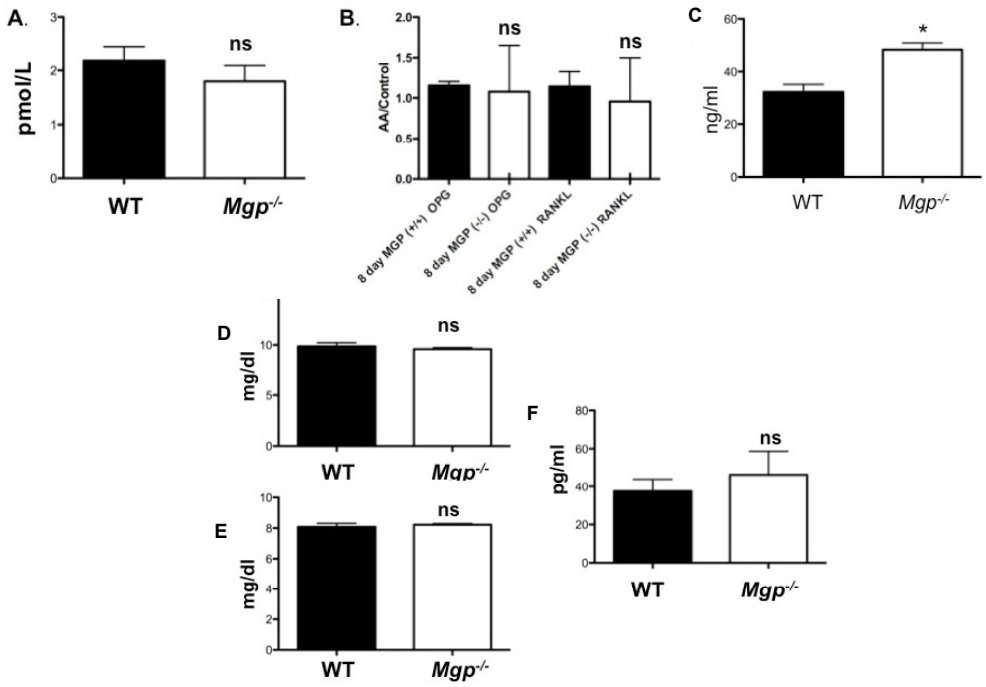

Figure 9
A) OPG serum ELISA in MGP wildtype and MGP-deficient mice reveal no significant differerence.(NS)
B) OPG and RANKL mRNA gene expression in both genotypes, results NS ($P > 0.05$).
C) Resorption analysis of osteoclasts by measuring CTX activity. ($P < 0.05$).
D) Serum calcium levels (n=4) NS
E) Serum Inorganic phosphate levels (n=4) NS
F) Serum PTH levels (n=3) NS
NS-Not Significant

TABEL 3		
PRIMER SEQUENCES	**Forward**	**Reverse**
MGP Wildtype allele	GCCACAATTTCTGCATCCTGC	CGGGAAAGATGAGGAAGAAGGG
MGP Mutant allele	TGCCTGAAGTAGCGGTTGTA	GAATGAACTGCAGGACGAGG
Twsg Wildtype allele	GCATCGCTTCTATCGCTTTC	TGAGGGATCCGCTGTAAGTC
Twsg Mutant allele	TTTTCTGAGACAACAGGGTTTC	CTGGTCTGCATTTGGGATCT
BSP	GAAACGGTTTCCAGTCCAG	CTGCATCTCCAGCCTTCTT
OCN	GAACAGACTCCGGCGCTA	AGGGAGGATCAAGTCCCG
OPG	ctgcctgggaagaagatcag	ttgtgaagctgtgcaggaac
RANKL	agccgagactacggcaagta	gcgctcgaaagtacaggaac
TRAP	CGTCTCTGCACAGATTGCA	GAGTTGCCACACAGCATCAC
DC-STAMP	GGGCACCAGTATTTTCCTGA	TGGCAGGATCCAGTAAAAGG
GAPDH	tgcaccaccaactgcttag	gatgcagggatgatgttc
L4	ccttctctggaacaaccttctcg	aagatgatgaacaccgaccttagc

TABLE 4
Parameters Evaluated in MGP and Twsg Mice

Trabecular Thickness	1D	Calculated as the averaged thickness of the trabeculae present in the field analyzed for the bone volume (
Trabcular Separation	1D	The closest distance horizontally between two neighboring trabeculae (mm)
Trabecular Number	1D	Evaluated as the number of trabeculae present in the field analyzed for the bone volume
Cortical Area	2D	Measurment evaluating the Cortical bone present in a saggital section midway through the bone (mm2)
Cortical Volume	3D	Cortical bone present in the femur (mm3)
Total Bone Volume	3D	Cortical and trabecular bone present in the femur (mm3)
Cortical Volume/Tissue Volume	3D	Cortical bone present in the femur (mm3) divided by the amount of marrow and bone present (mm3)
Cortcial Volume/Total Bone Volume	3D	Cortical bone present in the femur (mm3) divided by the combination of trabecular and cortical bone (mı
Bone Diameter	1D	Distance across the shaft at mid-diaphysis taken evaluatiing a cross sectional image (mm)
Cortical Width	1D	Distance across the cortical bone at mid-diaphysisevaluating a cross sectional image (mm)

REFERENCES

1. Wehrli, F., *Structural and mechanical assessment of trabecular bone by in vivo magnetic resonance imaging.* J Acoust Soc Am. **127**(3): p. 2031.
2. Lloyd, S.A., et al., *Spaceflight-relevant types of ionizing radiation and cortical bone: Potential LET effect?* Adv Space Res, 2008. **42**(12): p. 1889-1897.
3. Bobis, S., D. Jarocha, and M. Majka, *Mesenchymal stem cells: characteristics and clinical applications.* Folia Histochem Cytobiol, 2006. **44**(4): p. 215-30.
4. Krishnan, V., et al., *Osteogenesis in vitro: from pre-osteoblasts to osteocytes : A contribution from the Osteobiology Research Group, The Pennsylvania State University.* In Vitro Cell Dev Biol Anim. **46**(1): p. 28-35.
5. Solheim, E., *Growth factors in bone.* Int Orthop, 1998. **22**(6): p. 410-6.
6. Lee, M.H., et al., *BMP-2-induced Runx2 expression is mediated by Dlx5, and TGF-beta 1 opposes the BMP-2-induced osteoblast differentiation by suppression of Dlx5 expression.* J Biol Chem, 2003. **278**(36): p. 34387-94.
7. Gordon, J.A., et al., *Bone sialoprotein expression enhances osteoblast differentiation and matrix mineralization in vitro.* Bone, 2007. **41**(3): p. 462-73.
8. Bonewald, L.F. and M.L. Johnson, *Osteocytes, mechanosensing and Wnt signaling.* Bone, 2008. **42**(4): p. 606-15.
9. Feng, X., *Regulatory roles and molecular signaling of TNF family members in osteoclasts.* Gene, 2005. **350**(1): p. 1-13.
10. Hayman, A.R., et al., *Osteoclastic tartrate-resistant acid phosphatase (Acp 5): its localization to dendritic cells and diverse murine tissues.* J Histochem Cytochem, 2000. **48**(2): p. 219-28.
11. Yuan, F.L., et al., *The vacuolar ATPase in bone cells: a potential therapeutic target in osteoporosis.* Mol Biol Rep.
12. Tanaka, S., et al., *Role of RANKL in physiological and pathological bone resorption and therapeutics targeting the RANKL-RANK signaling system.* Immunol Rev, 2005. **208**: p. 30-49.

13. Takayanagi, H., *The role of NFAT in osteoclast formation.* Ann N Y Acad Sci, 2007. **1116**: p. 227-37.
14. Iwasaki, R., et al., *Cell fusion in osteoclasts plays a critical role in controlling bone mass and osteoblastic activity.* Biochem Biophys Res Commun, 2008. **377**(3): p. 899-904.
15. Yagi, M., et al., *Role of DC-STAMP in cellular fusion of osteoclasts and macrophage giant cells.* J Bone Miner Metab, 2006. **24**(5): p. 355-8.
16. Yagi, M., et al., *DC-STAMP is essential for cell-cell fusion in osteoclasts and foreign body giant cells.* J Exp Med, 2005. **202**(3): p. 345-51.
17. Daci, E., S. van Cromphaut, and R. Bouillon, *Mechanisms influencing bone metabolism in chronic illness.* Horm Res, 2002. **58 Suppl 1**: p. 44-51.
18. Heinrich, J., et al., *CSF-1, RANKL and OPG regulate osteoclastogenesis during murine tooth eruption.* Arch Oral Biol, 2005. **50**(10): p. 897-908.
19. Martin, T., J.H. Gooi, and N.A. Sims, *Molecular mechanisms in coupling of bone formation to resorption.* Crit Rev Eukaryot Gene Expr, 2009. **19**(1): p. 73-88.
20. Buckwalter, J.A., et al., *Bone biology. I: Structure, blood supply, cells, matrix, and mineralization.* Instr Course Lect, 1996. **45**: p. 371-86.
21. Kapustin, A. and C.M. Shanahan, *Targeting vascular calcification: softening-up a hard target.* Curr Opin Pharmacol, 2009. **9**(2): p. 84-9.
22. Xiao, Z., et al., *Analysis of the extracellular matrix vesicle proteome in mineralizing osteoblasts.* J Cell Physiol, 2007. **210**(2): p. 325-35.
23. Yagami, K., et al., *Matrix GLA protein is a developmental regulator of chondrocyte mineralization and, when constitutively expressed, blocks endochondral and intramembranous ossification in the limb.* J Cell Biol, 1999. **147**(5): p. 1097-108.
24. Giachelli, C.M., *Ectopic calcification: gathering hard facts about soft tissue mineralization.* Am J Pathol, 1999. **154**(3): p. 671-5.
25. Cancela, L., et al., *Molecular structure, chromosome assignment, and promoter organization of the human matrix Gla protein gene.* J Biol Chem, 1990. **265**(25): p. 15040-8.
26. Atzeni, F., P. Sarzi-Puttini, and M. Bevilacqua, *Calcium deposition and associated chronic diseases (atherosclerosis, diffuse idiopathic skeletal hyperostosis, and others).* Rheum Dis Clin North Am, 2006. **32**(2): p. 413-26, viii.

27. Atoda, H. and T. Morita, *A novel blood coagulation factor IX/factor X-binding protein with anticoagulant activity from the venom of Trimeresurus flavoviridis (Habu snake): isolation and characterization.* J Biochem, 1989. **106**(5): p. 808-13.
28. Shearer, M.J., *Role of vitamin K and Gla proteins in the pathophysiology of osteoporosis and vascular calcification.* Curr Opin Clin Nutr Metab Care, 2000. **3**(6): p. 433-8.
29. Rubinacci, A., *Expanding the functional spectrum of vitamin K in bone. Focus on: "Vitamin K promotes mineralization, osteoblast to osteocyte transition, and an anti-catabolic phenotype by {gamma}-carboxylation-dependent and -independent mechanisms".* Am J Physiol Cell Physiol, 2009. **297**(6): p. C1336-8.
30. Barone, L.M., et al., *Developmental expression and hormonal regulation of the rat matrix Gla protein (MGP) gene in chondrogenesis and osteogenesis.* J Cell Biochem, 1991. **46**(4): p. 351-65.
31. Cranenburg, E.C., L.J. Schurgers, and C. Vermeer, *Vitamin K: the coagulation vitamin that became omnipotent.* Thromb Haemost, 2007. **98**(1): p. 120-5.
32. Fraser, J.D. and P.A. Price, *Lung, heart, and kidney express high levels of mRNA for the vitamin K-dependent matrix Gla protein. Implications for the possible functions of matrix Gla protein and for the tissue distribution of the gamma-carboxylase.* J Biol Chem, 1988. **263**(23): p. 11033-6.
33. Lawton, D.M., et al., *Expression of the gene encoding the matrix gla protein by mature osteoblasts in human fracture non-unions.* Mol Pathol, 1999. **52**(2): p. 92-6.
34. Nishimoto, J.Z.a.S., *Matrix Gla Protein Gene Expression Is Elevated During Postnatal Development .* Matrix Biology, 1996. **15**: p. 131-140.
35. J. B. Ortiz-Delgado, D.C.S., C. S. B. Viegas and C.S. B. J. Scha, M. LCancela *Cloning of matrix Gla protein in a marine cartilaginous fish, Prionace glauca: preferential protein accumulation in skeletal and vascular systems.* Histochemistry Cell Biology, 2006. **126**(1): p. 89-101.
36. Gavaia, P.J., et al., *Osteocalcin and matrix Gla protein in zebrafish (Danio rerio) and Senegal sole (Solea senegalensis): comparative gene and protein expression during larval development through adulthood.* Gene Expr Patterns, 2006. **6**(6): p. 637-52.

37. Luo, G., *The matrix Gla protein gene is a marker of the chondrogenesis cell lineage during mouse development.* Journal of Bone and Mineral Research, 1995. **10**(2): p. 325-34.
38. Luo, G., et al., *Spontaneous calcification of arteries and cartilage in mice lacking matrix GLA protein.* Nature, 1997. **386**(6620): p. 78-81.
39. Steitz, S.A., et al., *Smooth muscle cell phenotypic transition associated with calcification: upregulation of Cbfa1 and downregulation of smooth muscle lineage markers.* Circ Res, 2001. **89**(12): p. 1147-54.
40. El-Maadawy, S., et al., *Cartilage formation and calcification in arteries of mice lacking matrix Gla protein.* Connect Tissue Res, 2003. **44 Suppl 1**: p. 272-8.
41. Persy, V. and P. D'Haese, *Vascular calcification and bone disease: the calcification paradox.* Trends Mol Med, 2009. **15**(9): p. 405-16.
42. Krueger, T., et al., *Coagulation meets calcification: the vitamin K system.* Int J Artif Organs, 2009. **32**(2): p. 67-74.
43. Munroe, P.B., et al., *Mutations in the gene encoding the human matrix Gla protein cause Keutel syndrome.* Nat Genet, 1999. **21**(1): p. 142-4.
44. Petryk, A., et al., *Twisted gastrulation and chordin inhibit differentiation and mineralization in MC3T3-E1 osteoblast-like cells.* Bone, 2005. **36**(4): p. 617-26.
45. Mason, E.D., et al., *Dorsal midline fate in Drosophila embryos requires twisted gastrulation, a gene encoding a secreted protein related to human connective tissue growth factor.* Genes Dev, 1994. **8**(13): p. 1489-501.
46. Nosaka T, M.S., Kitamura H, Nakajima H, Shibata F, Morikawa Y, Kataoka Y, Ebihara Y, Kawashima T, Itoh T, Ozaki K, Senba E, Tsuji K, Makishima F, Yoshida N, Kitamura T, *Mammalian Twisted Gastrulation Is Essential for Skeleto-Lymphogenesis*

. MOLECULAR AND CELLULAR BIOLOGY, 2003. **23**(8).
47. Petryk, A., et al., *The mammalian twisted gastrulation gene functions in foregut and craniofacial development.* Dev Biol, 2004. **267**(2): p. 374-86.
48. Zakin, L. and E.M. De Robertis, *Inactivation of mouse Twisted gastrulation reveals its role in promoting Bmp4 activity during forebrain development.* Development, 2004. **131**(2): p. 413-24.

49. Melnick M, P.A., Abichaker G, Witcher D, Person AD, Jaskoll T., *Embryonic salivary gland dysmorphogenesis in Twisted gastrulation deficie.* Arch Oral Biol. , 2006. **51**(5): p. 433-38.
50. Little, S.C. and M.C. Mullins, *Twisted gastrulation promotes BMP signaling in zebrafish dorsal-ventral axial patterning.* Development, 2004. **131**(23): p. 5825-35.
51. Jensen, E.D., et al., *Bone morphogenic protein 2 directly enhances differentiation of murine osteoclast precursors.* J Cell Biochem. **109**(4): p. 672-82.
52. Weischaus E, N.-V.C., Jurgens G and *Mutations affecting the pattern of the larval cuticle in Drosophila Malanogaster.* Wilhelm Roux's Arch. Dev. Biol, 1984. **193**: p. 296-307.
53. Ross JJ, S.O., Vilmos P, Petryk A, Kim H, Gaudenz K, Hermanson S, Ekker SC, O'Connor MB, *Twisted gastrulation is a conserved extracellular BMP antagonist.* Nature, 2001. **410**(6827): p. 479-83.
54. Nosaka T, M.S., Kitamura H, Nakajima H, Shibata F, Morikawa Y, Kataoka Y, Ebihara Y, and I.T. Kawashima T, Ozaki K, Senba E, Tsuji K, Makishima F, Yoshida N, Kitamura T *Mammalian twisted gastrulation is essential for skeleto-lymphogenesis.* Mol Cell Biol 2003. **23**(8): p. 2969-80.
55. Gazzerro E, D.V., Stadmeyer L, Gale NW, Economides AN, Canalis E *Twisted gastrulation, a bone morphogenetic protein agonist/antagonist, is not required for post-natal skeletal function.* Bone, 2006. **39**(6): p. 1252-60.
56. Chang C, H.D., Chau S, Chickering T, Woolf EA, Holmgren LM, Bodorova J, Gearing DP, , *Twisted gastrulation can function as a BMP antagonist. .* Nature, 2001. **410**(6827): p. 483-7.
57. Oelgeschlager, M., et al., *The evolutionarily conserved BMP-binding protein Twisted gastrulation promotes BMP signalling.* Nature, 2000. **405**(6788): p. 757-63.
58. Larrain J, O.M., Ketpura NI, Reversade B, Zakin L, De Robertis EM, *Proteolytic cleavage of Chordin as a switch for the dual activities of Twisted gastrulation in BMP signaling..* Development, 2001. **128**(22): p. 4439-47.
59. Scott IC, B.I., Pappano WN, Maas SA, Cho KW, Greenspan DS *Homologues of Twisted gastrulation are extracellular cofactors in antagonism of BMP signalling.* Nature, 2001. **410**(6827): p. 475-8.

60. Piccolo, S., et al., *Cleavage of Chordin by Xolloid metalloprotease suggests a role for proteolytic processing in the regulation of Spemann organizer activity.* Cell, 1997. **91**(3): p. 407-16.
61. Shimmi, O. and M.B. O'Connor, *Physical properties of Tld, Sog, Tsg and Dpp protein interactions are predicted to help create a sharp boundary in Bmp signals during dorsoventral patterning of the Drosophila embryo.* Development, 2003. **130**(19): p. 4673-82.
62. Sotillo Rodriguez JE, M.K., Jensen ED, Carlson AE, Schwarz T, Pham L, MacKenzie B, Prasad H, Rohrer MD, Petryk A, Gopalakrishnan R., *Enhanced osteoclastogenesis causes osteopenia in twisted gastrulation-deficient mice through increased BMP signaling.* J Bone Miner Res, 2009. **24**(11): p. 1917-26.
63. Sharma, S.M., et al., *MITF and PU.1 recruit p38 MAPK and NFATc1 to target genes during osteoclast differentiation.* J Biol Chem, 2007. **282**(21): p. 15921-9.
64. Rozen, S. and H. Skaletsky, *Primer3 on the WWW for general users and for biologist programmers.* Methods Mol Biol, 2000. **132**: p. 365-86.
65. Hotokezaka, H., et al., *Molecular analysis of RANKL-independent cell fusion of osteoclast-like cells induced by TNF-alpha, lipopolysaccharide, or peptidoglycan.* J Cell Biochem, 2007. **101**(1): p. 122-34.
66. Raisz, L.G., *Pathogenesis of osteoporosis: concepts, conflicts, and prospects.* J Clin Invest, 2005. **115**(12): p. 3318-25.
67. Solomon, D.H., L. Rekedal, and S.M. Cadarette, *Osteoporosis treatments and adverse events.* Curr Opin Rheumatol, 2009. **21**(4): p. 363-8.
68. Doherty TM, A.K., Fitzpatrick LA, Qiao JH, Wilkin DJ, Detrano RC, Dunstan CR, Shah PK, Rajavashisth TB, *Calcification in atherosclerosis: bone biology and chronic inflammation at the arterial crossroads.* Proc Natl Acad Sci U S A, 2003. **100**(20): p. 11201-6.
69. Jie, K.G., et al., *Vitamin K status and bone mass in women with and without aortic atherosclerosis: a population-based study.* Calcif Tissue Int, 1996. **59**(5): p. 352-6.
70. Moon, J., B. Bandy, and A.J. Davison, *Hypothesis: etiology of atherosclerosis and osteoporosis: are imbalances in the calciferol endocrine system implicated?* J Am Coll Nutr, 1992. **11**(5): p. 567-83.

71. Tintut, Y. and L.L. Demer, *Recent advances in multifactorial regulation of vascular calcification.* Curr Opin Lipidol, 2001. **12**(5): p. 555-60.
72. van Summeren, M.J., et al., *Calcinosis in juvenile dermatomyositis: a possible role for the vitamin K-dependent protein matrix Gla protein.* Rheumatology (Oxford), 2008. **47**(3): p. 267-71.
73. Browner, W.S., et al., *Non-trauma mortality in elderly women with low bone mineral density. Study of Osteoporotic Fractures Research Group.* Lancet, 1991. **338**(8763): p. 355-8.
74. Ceriello, A. and E. Motz, *Is oxidative stress the pathogenic mechanism underlying insulin resistance, diabetes, and cardiovascular disease? The common soil hypothesis revisited.* Arterioscler Thromb Vasc Biol, 2004. **24**(5): p. 816-23.
75. Chau, D.L., S.V. Edelman, and M. Chandran, *Osteoporosis and diabetes.* Curr Diab Rep, 2003. **3**(1): p. 37-42.
76. Hermans, M.M., et al., *Undercarboxylated matrix GLA protein levels are decreased in dialysis patients and related to parameters of calcium-phosphate metabolism and aortic augmentation index.* Blood Purif, 2007. **25**(5-6): p. 395-401.
77. Morrow, J.D., *Quantification of isoprostanes as indices of oxidant stress and the risk of atherosclerosis in humans.* Arterioscler Thromb Vasc Biol, 2005. **25**(2): p. 279-86.
78. Rigalleau, V., et al., *Bone loss in diabetic patients with chronic kidney disease.* Diabet Med, 2007. **24**(1): p. 91-3.
79. Rubin, M.R. and S.J. Silverberg, *Vascular calcification and osteoporosis--the nature of the nexus.* J Clin Endocrinol Metab, 2004. **89**(9): p. 4243-5.
80. Barengolts, E.I., et al., *Osteoporosis and coronary atherosclerosis in asymptomatic postmenopausal women.* Calcif Tissue Int, 1998. **62**(3): p. 209-13.
81. Horiuchi, M., et al., *Upregulation of vascular extracellular superoxide dismutase in patients with acute coronary syndromes.* Arterioscler Thromb Vasc Biol, 2004. **24**(1): p. 106-11.
82. Parker, B.D., et al., *Association of kidney function and uncarboxylated matrix Gla protein: data from the Heart and Soul Study.* Nephrol Dial Transplant, 2009. **24**(7): p. 2095-101.

83. Hmamouchi, I., et al., *Low bone mineral density is related to atherosclerosis in postmenopausal Moroccan women.* BMC Public Health, 2009. **9**: p. 388.
84. Kiel, D.P., et al., *Bone loss and the progression of abdominal aortic calcification over a 25 year period: the Framingham Heart Study.* Calcif Tissue Int, 2001. **68**(5): p. 271-6.
85. Schulz, E., et al., *Aortic calcification and the risk of osteoporosis and fractures.* J Clin Endocrinol Metab, 2004. **89**(9): p. 4246-53.
86. Uyama, O., et al., *Bone changes and carotid atherosclerosis in postmenopausal women.* Stroke, 1997. **28**(9): p. 1730-2.